Updating hierarchical 3D models for P&ID purposes using LiDAR point clouds

Marek Baścik [1], Artur Warchoł [2]

[1] 3Deling Sp. z o.o., Kraków, Poland - marek.bascik@3deling.com
[2] Department of Geodesy and Geomatics, Faculty of Environmental Engineering, Geomatics and Renewable Energy, Kielce University of Technology, Kielce, Poland - awarchol@tu.kielce.pl

Keywords: point clouds, 3D models, Piping and Instrumentation Diagram, PDMS, LiDAR.

Abstract

This publication presents a solution for comprehensive TLS data processing, verification and documentation preparation. The WEBPANO platform allows for the integration of 3D models with P&ID diagrams, external documentation, point clouds and panoramic images. The research part verified the accuracy between the 3D model developed according to the proposed scheme and the point cloud.

1. Introduction

1.1 Point clouds and modeling

LiDAR laser scanning has been a reliable and fast technology for acquiring geospatial data for many years. Depending on the data acquisition ceiling (ALS/ULS, MLS or TLS), we obtain data with different characteristics. The most precise and dense are, of course, TLS data sets. High density allows for the collection of highly detailed data on the geometry of objects. Such solutions are most often used in inventory measurements of objects for which there is no documentation due to their age (e.g. HBIM) or in situations where the object differs significantly from the last available documentation. Industrial objects (factories, production plants or refineries) and ship engine rooms are also interesting cases. These are objects with a high saturation of infrastructure, where both uninterrupted operation and the possibility of making changes to the installation are of key importance. For this reason, there is a need to provide high-quality spatial data in the form of point clouds that are able to accurately represent the plant's space in digital form.

In addition to environmental (Sobura, Kapusta, 2024) or forestry (Krok et al., 2020), (Balestra et al. 2024) or offshore (Kogut et al., 2022), LiDAR data are very often used in architecture or for inventory purposes of various objects (Sobura et. al., 2023), (Warchoł, 2015), (Damięcka-Suchocka et al., 2022), to create 3D BIM models of existing objects (Gruner et al., 2022), (Borkowski, Kubrat, 2024), mining (Blachowski et al., 2024), tourism (Bieda et al., 2021) or 3D cadaster (Grzelka et al., 2024). To speed up data acquisition, mobile laser scanning (MLS) can be used for objects for which the required accuracy is lower. Examples of applications of this technology in various fields are as follows: (Di Stefano et al., 2021), (Warchoł et al., 2023), (Wysocki et al., 2024) urban environment, (Adamek et al., 2024) mining or the low-cost version (Mitka et al., 2024) or (Trybała et al., 2023).
In addition to their numerous advantages, point clouds also have certain disadvantages, which are mentioned in the paper (Warchoł et al., 2024).

P&ID (Piping and Instrumentation Diagram) is one of the most important technical documents in industry. It is used in the design, construction and maintenance of industrial installations – refineries, chemical plants and other industrial facilities. These diagrams show pipelines, fittings, process equipment, and measurement and control systems. They serve as a flat map of the installation, allowing engineers and operators to understand how the entire system works. They are essential for planning upgrades, operating and ensuring safety.

P&IDs are a common language for engineers of various specialities. Thanks to them, designers, contractors and maintenance services work on the basis of a single, consistent set of information presented in graphical form.

Although P&ID documentation is extremely important, in practice it is rarely up to date. Physical changes to the installation – replacement of a valve, addition of a section of pipeline or modification of the control system – are not always reflected in the diagrams available.

The most common reasons for this are:
- lack of time and resources,
- responsibility spread across teams,
- documentation kept in paper form or in inflexible PDF/CAD files.

The result of this situation is serious and, over time, increasing discrepancies between the diagrams and the actual state of the installation. This increases the risk of errors, delays and problems during audits and compliance reviews – especially in crisis situations when a component of the installation needs to be redesigned quickly in the event of a failure.

1.2 Solution

To address the above issues, a solution has been developed which, based on LiDAR point clouds, allows for the updating of hierarchical 3D models (including industrial installations) and their integration with 2D documentation (P&ID). An additional advantage of this solution is the ability to simultaneously display LiDAR point clouds, 3D models, meshes or spherical photos in the WebPano browser, together with a preview of P&ID documentation (Fig. 1 and Fig. 2).

Marking an element in the WebPano environment generates a link to the object in the P&ID diagram, making it possible to point/search in both directions, i.e. an element marked in the

P&ID diagram appears, for example, on the model (WebPano environment), but you can also select an object in WebPano (point cloud, mesh or 3D BIM model) and the software will highlight it on the P&ID diagram (Fig. 1).

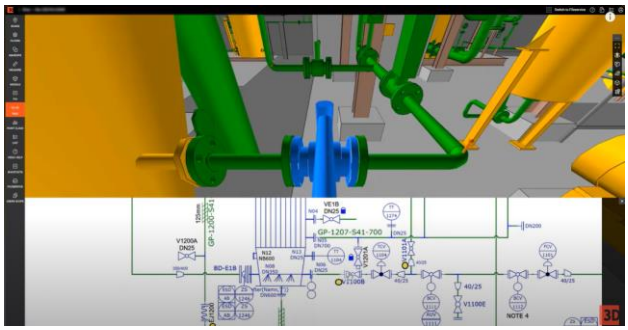

Figure 1. P&ID with 3D model in WebPano – selected object in blue.

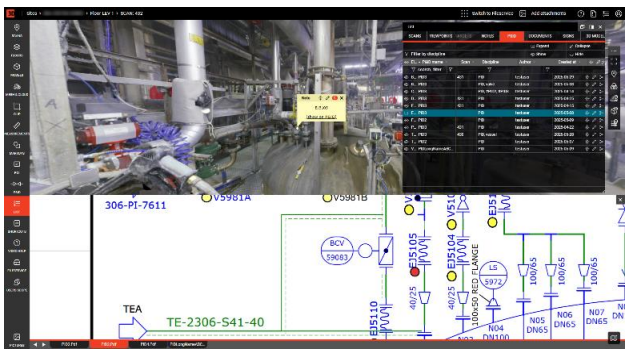

Figure 2. P&ID with point cloud in WebPano.

The above drawings present the effect, but the process of creating a multifunctional model requires more complex tools. Due to shortcomings in the software and the desire to create a uniform, consistent and compatible process, it was decided to develop proprietary tools to perform the above tasks. The process of creating a hierarchical 3D model is shown schematically in Fig. 3.

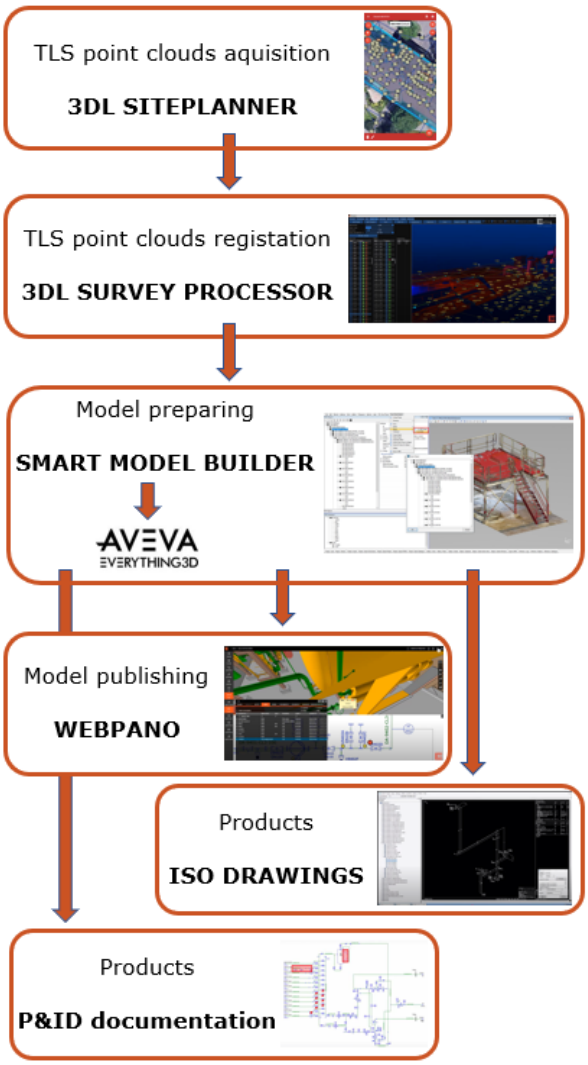

Figure 3. Workflow of the modelling and documentation process with names of used software.

The development of proprietary software for solving specific issues from Fig. 3 (SITEPLANNER, PROCESSOR, SMART MODEL BUILDER, WEBPANO) allows for the adaptation of functionality to the specific nature of the projects being carried out and ensures a reliable workflow.

The effectiveness of the measurement stage using SITEPLANNER + PROCESSOR is presented in the publication (Warchoł, Baścik, Pietrzyk, 2024). This text presents the innovative Smart Model Builder (SMB) tool designed to create hierarchical models in a CAD (Computer-Aided Design) environment. This tool aims to streamline the process of modelling objects in the context of engineering projects by simplifying the structuring of data in 3D models.
Depending on the purpose of the model and the expected end product, a 3D environment appropriate for the type of project is selected. For the simplest tasks, CAD solutions work very well due to their ease of use in modelling and their widespread application, which also translates into the experience of those who use them.

In the case of more advanced Plant/PDMS models, which extend CAD designs with a hierarchical model structure and

intelligent objects such as catalogue elements, the situation becomes much more complicated.

1.3 Model preparing with SMB

Smart Model Builder (SMB) enables the development of models with a complex hierarchical structure based on simple solids created in the MicroStation environment, which allows for easier management of complex projects, especially when the project requires the integration of many elements or components. Smart Model Builder, as a plugin that extends the functionality of MicroStation, allows you to model simple solids and organise them into a hierarchical structure. In addition, it allows you to add catalogue objects, which significantly increases flexibility in creating more complex models.

A series of key functionalities that make up a complete solution to the problem is presented using a real-life example of the transition from a discrete representation of an object in the form of a LiDAR point cloud, through the creation of simple solid objects with names, to export to a text file and finally import to the E3D (AVEVA) environment – figures 4 to 8.

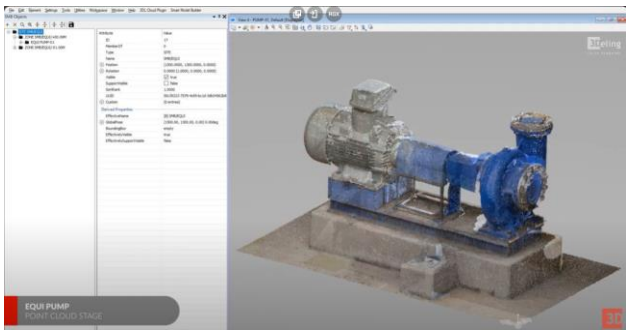

Figure 4. Point cloud of EQUI PUMP coloured by RGB values.

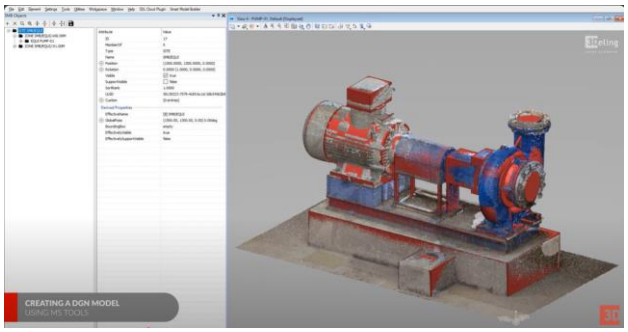

Figure 5. Creating DGN model using MicroStation tools – red object.

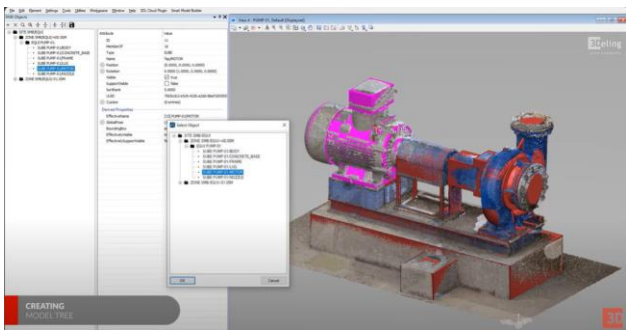

Figure 6. Creating model tree in SBM.

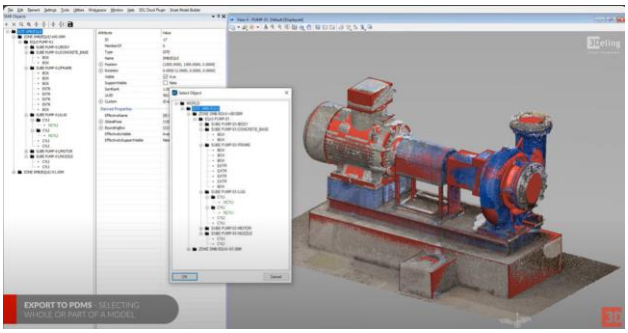

Figure 7. Export to PDMS – selecting whole or a part of a model.

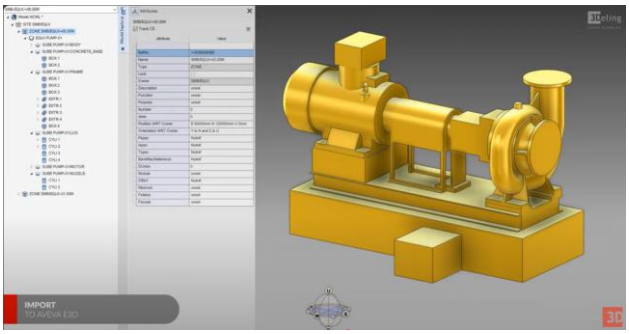

Figure 8. Import to AVEVA E3D.

An additional advantage is the integration of P&ID in WebPano, which allows P&ID diagrams to be linked to spatial object data – a 3D model (Fig. 1) or a point cloud (Fig. 2).

What is more, P&IDs can be updated in this process based on LiDAR point clouds, so that the documentation always reflects the actual state of the plant, and at the same time it is not necessary to create the entire model. The user can link P&ID elements with the corresponding objects themselves in WebPano. This allows the valve or pump symbol in the diagram to become a reference to the real object in the plant space. It is also possible to add notes to the objects (fig. 9).

Figure 9. Object with note in WebPano.

2. Materials and methods

For detailed analyses of modelling accuracy, one station from a larger TLS project was selected, for which a 3D model was also prepared according to the diagram in Fig. 3. The differences between the TLS cloud and the model were calculated using 3Deling software. Their spatial distribution for one of the stations was saved in the form of raster files. The station

included in the analysis consists of 6 difference files – 4 in the directions of the cardinal points, one upwards, i.e. the ceiling, and one downwards, i.e. the floor. The visualisation of the differences can be seen in Fig. 10, where the largest differences (125 mm) are marked in red and blue, respectively, -125 mm in red and +125 mm in blue, while differences close to zero are shown in yellow and green.

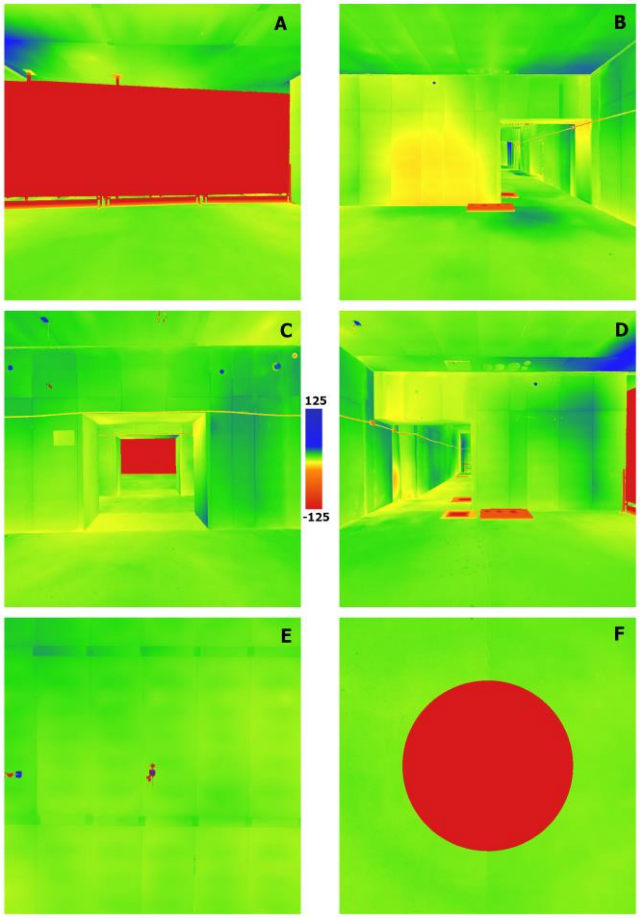

Figure 10. Six images from one scan position with differences in mm between point cloud and the model. Fig. A-D – side views, E – top view – ceiling, F – floor.

The frequency of occurrence of individual differences from Fig. 10 is presented using histograms in Fig. 11.

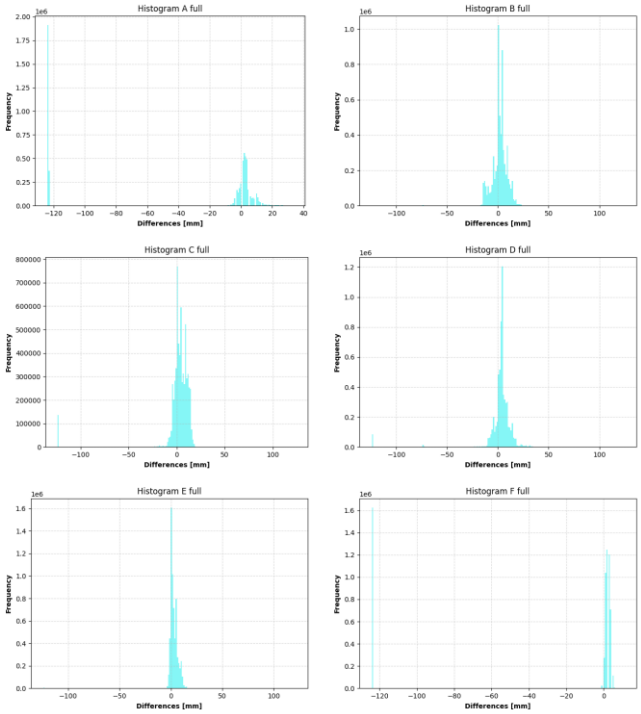

Figure 11. Histograms from the full difference package for the difference images from Fig. 10.

When analysing histograms from the full set of differences for each image, it is difficult to reliably assess the accuracy of the model itself due to a certain number of pixels for which there are large differences between the cloud and the model. These differences are not due to the low quality of the model, but to the presence of unmodelled objects on the cloud. These include, for example, temporary construction elements, work partitions, pallets of building materials or packaging. In this particular case, where the goal was to model an object consisting of walls, floors and ceilings, unmodelled elements also include installations.

For this reason, the difference packages ranging from -125 mm to +125 mm were divided into 5 classes in accordance with the legend attached to Fig. 11. The selection of classes was dictated by the control methodology. Class 3, which includes differences ranging from -30 mm to +30 mm, consists of fragments modelled in accordance with the design requirements. Classes 2 and 4, with values ranging from -100 mm to -30 mm and from 30 mm to 100 mm, are locations ‘suspected of gross errors’ that should be checked by the operator supervising the work. The range from -125 mm to -100 mm and from 100 mm to 125 mm are locations where objects appear in the cloud but are not present in the model.

Histograms of differences and values characterising individual ranges have been prepared for each class.

3. Results

Taking into account the assumptions made in the previous chapter, the differences in Fig. 10 were divided into five classes according to their values. The spatial distribution of class membership is shown in Fig. 12.

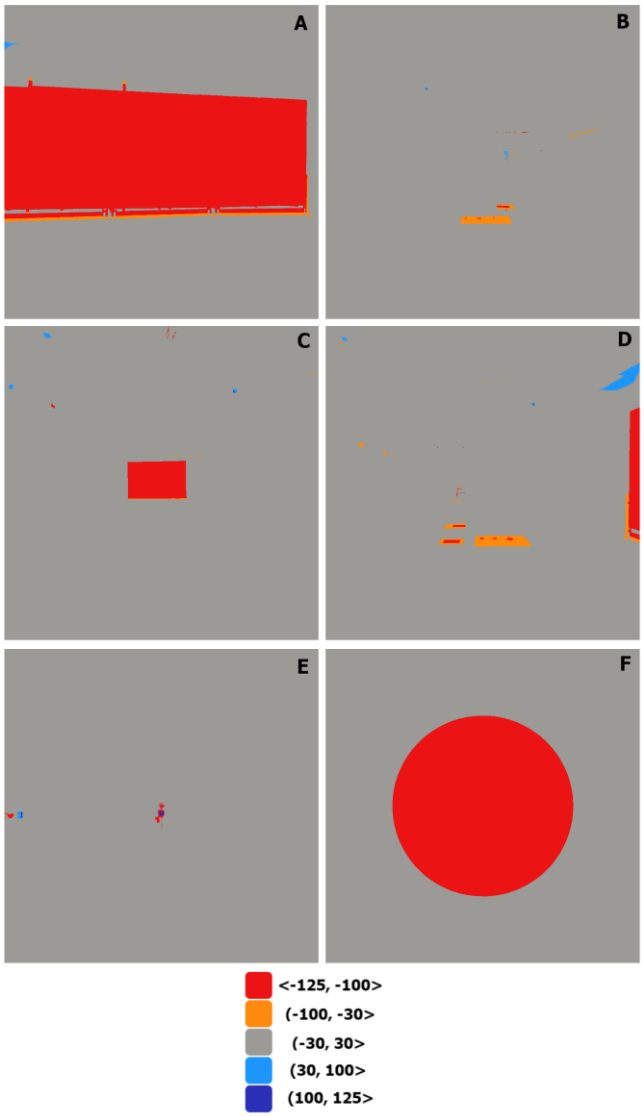

Figure 12. Spatial distribution of class membership

The first and last classes, red and navy blue respectively, contain the greatest differences, i.e. places where unmodelled objects occur. These are elements that are recorded in the point cloud but are not subject to modelling due to the design assumptions.

Classes two and four, orange and light blue respectively, contain differences exceeding the assumed accuracy of the model. This range is an area of particular interest to the person controlling the model.

Due to the use of images for model quality control and the specific viewing point of the object, this class contains pixels with large differences at the junction of key classes – 'within tolerance' and 'unmodelled' – which the operator must assess independently to determine whether they are large modelling errors or fragments of an unmodelled object.

The last is the third class – grey, which contains the area that meets the accuracy requirements of the project. Analysing the histograms of the third class (grey) – Fig. 13, it can be seen that their shape resembles a Gaussian curve. They also do not appear to be 'cut out' from a larger data set, as their frequency, visible on the histogram, drops significantly in the range of -10 mm to +10 mm/+20 mm.

In the histograms shown in Fig. 14, the frequency of occurrence of individual differences is not regular, but is closely related to the number of unmodelled elements. Quantitatively, it can be considered that there are not many such points, as there are hundreds or thousands of deviations, while in the 'grey' class (Fig. 13) there are hundreds of thousands or even millions of them. The absence of histogram F in Fig. 14 is due to the lack of differences in this class for image F.

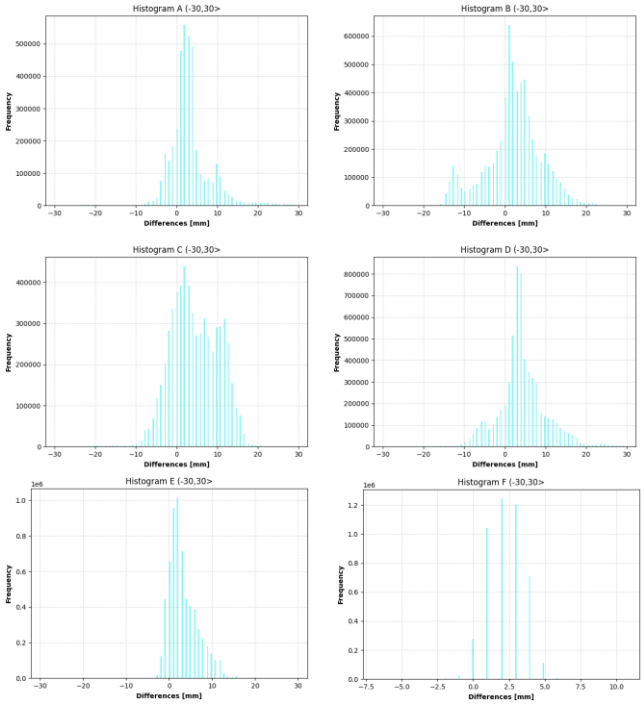

Figure 13. Histograms of third (grey) class.

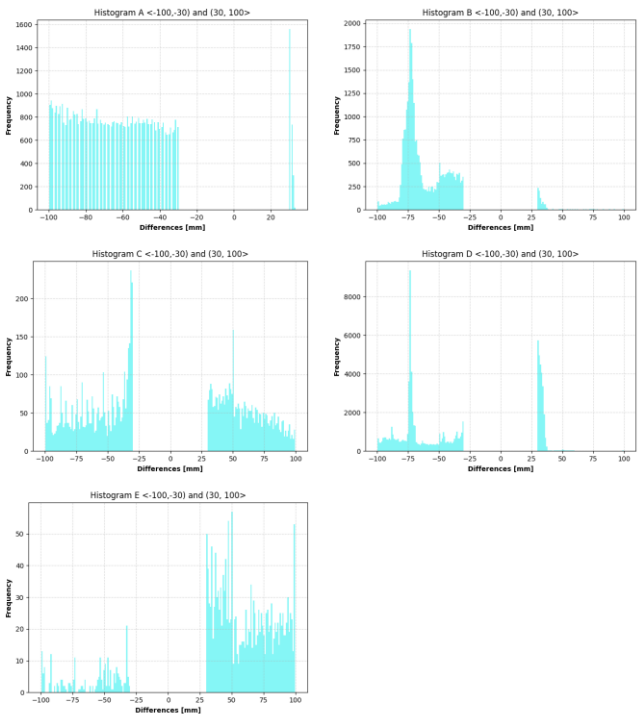

Figure 14. Histograms of second and fourth "to check" class.

The combined histograms for the first and fifth classes are shown in Fig. 15. The number of differences is high, e.g. Fig. 15 A shows approx. 2 million out of 6,250,000 total image points, but this is justified by a large unmodelled object – a temporary construction partition.

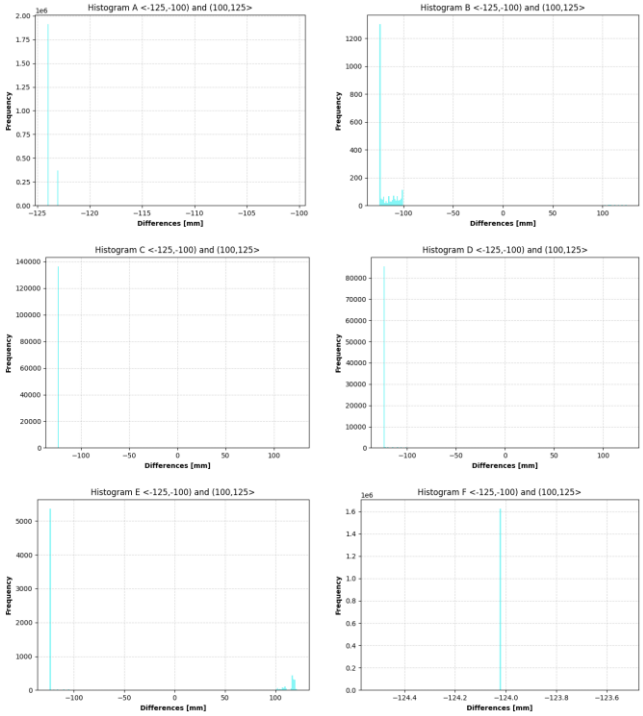

Figure 15. Histograms of first and fifth class – "not for modelling".

The validity of eliminating differences for non-modelled objects is also evident in the values characterising individual images – mean, median and standard deviation. The values for images A–F from the full data set (Table 1) and only from the third class, grey (-30.30> - Table 2, are summarised below. As can be seen in the above table, in all cases A-F there was an improvement in standard deviation.

Full data set	Mean [mm]	Median [mm]	Std. dev. [mm]
A	-44,18	0,00	61,26
B	1,66	1,95	8,49
C	1,57	3,91	19,82
D	1,74	3,91	17,77
E	3,12	1,95	5,43
F	-30,61	1,95	55,40

Table 1. Values characterising the difference sets for the complete data set – as in Fig. 11.

Third class (-30,30>	Mean [mm]	Median [mm]	Std. dev. [mm]
A	3,13	2,93	5,20
B	1,99	1,95	6,80
C	4,39	3,91	5,92
D	4,09	3,91	6,02
E	3,19	1,95	3,32
F	2,23	1,95	1,23

Table 2. Values characterising the difference sets for third class – as in Fig. 13.

As can be seen in the above table, in all cases A-F there was an improvement in standard deviation.

4. Conclusions

Integration also works when only a point cloud is available, which is much less expensive and faster than a 3D model solution.
The traditional approach, i.e. manual editing of CAD or PDF files, is a time-consuming process, prone to errors and difficult to verify. With the approach using WebPano and 3D scanning, we obtain:
- Objectivity of data – the scan reflects the actual condition of the installation.
- Centralised online access – all team members work on the same data.
- Integration of information – schematic documentation is directly linked to spatial information.
- Transparency of changes – each update is visible and easy to document.
- Remote updating – thanks to data from the scanner and the efficient WebPano platform, diagrams can be updated remotely, without the need for physical presence at the facility.

P&ID integration in WebPano is a step towards building complete digital twins of industrial installations. Up-to-date schematics, linked to spatial data, provide a solid foundation for implementing monitoring, prediction and optimisation of plant operations.

Significant differences appear in the image of differences when objects are scanned in the field and then some of them are not modelled. It is not always possible to completely empty an object, so such situations may occur. Therefore, the operator's decision is needed to analyse the distribution of differences: is the difference large because there is an object in the cloud that we are not modelling, or is the model actually inaccurate?

Assessing the quality of the model based solely on histograms from complete data is inadequate and may distort the conclusions drawn.

Standard deviation could be used for selecting images with many unmodelled elements

References

Sobura, S.; Kapusta, Ł. 2024: Assesing the Potential of Digital Terrain Models for Monitoring Additional Subsidence of Communication Embankments in Mining Areas—A Case Study. Struct. Environ., 16, 84–96.

Krok, G.; Kraszewski, B.; Stereńczak, K. 2020: Application of Terrestrial Laser Scanning in Forest Inventory—An Overview of Selected Issues. For. Res. Pap., 81, 175–194.

Balestra, M.; Marselis, S.; Sankey, T.T.; Cabo, C.; Liang, X.; Mokroš, M.; Peng, X.; Singh, A.; Stereńczak, K.; Vega, C.; et al. 2024: LiDAR Data Fusion to Improve Forest Attribute Estimates: A Review. Curr. For. Rep., 10, 281–297.

Sobura, S.; Bacharz, K.; Granek, G. 2023: Analysis of two-option integration of unmanned aerial vehicle and terrestrial laser scanning data for historical architecture inventory. Geod. Cartogr., 49, 76–87.

Warchoł, A. 2015: Analysis of Possibilities to Registration TLS Point Clouds without Targets on the Example of the Castle Bridge in Rzeszów. In Proceedings of the International Multidisciplinary Scientific GeoConference Surveying Geology and Mining Ecology Management (SGEM 2015), Albena, Bulgaria, 18–24 June 2015

Damięcka-Suchocka, M.; Katzer, J.; Suchocki, C. 2022: Application of TLS Technology for Documentation of Brickwork Heritage Buildings and Structures. Coatings, 12, 1963.

Gruner, F.; Romanschek, E.; Wujanz, D.; Clemen, C. 2022: Co-Registration of Tls Point Clouds With Scan-Patches and Bim-Faces. Int. Arch. Photogramm. Remote Sens. Spat. Inf. Sci.—ISPRS Arch., 46, 109–114.

Skrzypczak, I.; Oleniacz, G.; Leśniak, A.; Zima, K.; Mrówczyńska, M.; Kazak, J.K. 2022: Scan-to-BIM Method in Construction: Assessment of the 3D Buildings Model Accuracy in Terms Inventory Measurements. Build. Res. Inf., 50, 859–880.

Borkowski, A.S.; Kubrat, A. 2024: Integration of Laser Scanning, Digital Photogrammetry and BIM Technology: A Review and Case Studies. Eng, 5, 2395–2409.

Blachowski, J.; Wajs, J.; Walerysiak, N.; Becker, M. 2024: Monitoring of Post-Mining Subsidence Using Airborne and Terrestrial Laser Scanning Approach. Arch. Min. Sci., 69, 431–446.

Bieda, A.; Balawejder, M.; Warchoł, A.; Bydłosz, J.; Kolodiy, P.; Pukanská, K. 2021: Use of 3D Technology in Underground Tourism: Example of Rzeszow (Poland) and Lviv (Ukraine). Acta Montan. Slovaca, 26, 205–221.

Grzelka, K.; Pargieła, K.; Jasińska, A.; Warchoł, A.; Bydłosz, J. 2024: Registration of Objects for 3D Cadastre: An Integrated Approach. Land, 13, 2070.

Di Stefano, F.; Chiappini, S.; Gorreja, A.; Balestra, M.; Pierdicca, R. 2021: Mobile 3D Scan LiDAR: A Literature Review. Geomat. Nat. Hazards Risk, 12, 2387–2429.

Warchoł, A.; Karaś, T.; Antoń, M. 2023: Selected Qualitative Aspects of Lidar Point Clouds: Geoslam Zeb-Revo and Faro Focus 3D X130. Int. Arch. Photogramm. Remote Sens. Spat. Inf. Sci.—ISPRS Arch., 48, 205–212.

Wysocki, O.; Hoegner, L.; Stilla, U. 2024: MLS2LoD3: Refining Low LoDs Building Models with MLS Point Clouds to Reconstruct Semantic LoD3 Building Models. In Recent Advances in 3D Geoinformation Science; Springer Nature: Cham, Switzerland; pp. 367–380.

Adamek, A.; Będkowski, J.; Kamiński, P.; Pasek, R.; Pełka, M.; Zawiślak, J. 2024: Method for Underground Mining Shaft Sensor Data Collection. Sensors, 24, 4119.

Mitka, B.; Klapa, P.; Gawronek, P. 2024: Laboratory Tests of Metrological Characteristics of a Non-Repetitive Low-Cost Mobile Handheld Laser Scanner. Sensors, 24, 6010.

Trybała, P.; Kasza, D.; Wajs, J.; Remondino, F. 2023: Comparison of Low-Cost Handheld Lidar-Based Slam Systems for Mapping Underground Tunnels. Int. Arch. Photogramm. Remote Sens. Spat. Inf. Sci.—ISPRS Arch. 2023, 48, 517–524.

Warchoł, A.; Pęzioł, K.; Baścik, M. 2024: Energy-Saving Geospatial Data Storage—LiDAR Point Cloud Compression. Energies, 17, 6413.

Kogut, T.; Tomczak, A.; Słowik, A.; Oberski, T. 2022: Seabed Modelling by Means of Airborne Laser Bathymetry Data and Imbalanced Learning for Offshore Mapping. Sensors, 22, 3121

Warchoł A., Baścik M., Pietrzyk A., 2024: TLS measurement automation – case study SITEPLANNER. *Geoinformatica Polonica*, vol. 23, 113-120. doi.org/10.4467/21995923GP.24.009.20901